Bioconjugate Chemistry

Article

pubs.acs.org/bc

PNA–Rose Bengal Conjugates as Efficient DNA Photomodulators

Yossi Shemesh and Eylon Yavin*

The Institute for Drug Research, The School of Pharmacy, The Hebrew University of Jerusalem, Hadassah Ein-Kerem, Jerusalem 91120, Israel

Supporting Information

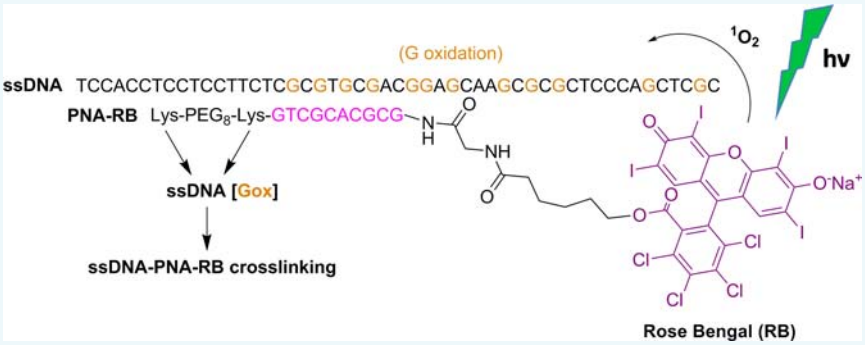

ABSTRACT: Selective photoinduced modulation of DNA may provide a powerful therapeutic tool allowing spatial and temporal control of the photochemical reaction. We have explored the photoreactivity of peptide nucleic acid (PNA) conjugates that were conjugated to a highly potent photosensitizer, Rose Bengal (RB). In addition, a short PEGylated peptide (K-PEG_8-K) was conjugated to the C-terminus of the PNA to improve its water solubility. A short irradiation (visible light) of PNA conjugates with a synthetic DNA resulted in highly efficient photomodulation of the DNA as evidenced by polyacrylamide gel electrophoresis (PAGE). In addition, a PNA-RB conjugate replacing K-PEG_8-K with four L-glutamic acids (E_4) was found to be photoinactive. Irradiation of active PNA-RB conjugates with synthetic DNA in D_20 augments the photoactivity; supporting the involvement of singlet oxygen. PAGE, HPLC, and MALDI-TOF analyses indicate that PNA-DNA photo-cross-linking is a significant pathway in the observed photoreactivity. Selective photo-cross-linking of such PNA-RB conjugates may be a novel approach to selective photodynamic therapy (sPDT) as such molecules would be sequence-specific, cell-permeable, and photoactivated in the visible region.

INTRODUCTION

Selective photomodulation of DNA has been considered as an alternative approach to control gene expression in a timely and persistent manner. In recent years, several elegant studies have shown that interstrand photo-cross-linking (ICL) of a designed oligomer targeting a complementary DNA strand is achievable by photolysis in the UV region.[1−9] Other approaches to DNA photomodulation include the activation of a furanyl modified oligomer by an external photosensitizer (PS)[10] and by ruthenium-tethered oligomers that are photoactivated by visible light (442 nm).[11]

For such an approach to be feasible as a therapeutic one, several requirements should be considered: (1) the light source should be tissue permeable and nontoxic, (2) the oligomer of choice should be cell permeable and, (3) binding to DNA should lead to sequence-specific DNA photomodulation.

In this regard, photodynamic therapy (PDT), which involves the administration of photosensitizing drugs and subsequent exposure of the tissue to light, has emerged as a novel clinical approach for the treatment of various tumors and some other nonmalignant conditions.[12] Due to the selectivity of drug uptake and the control of light delivery, PDT has the potential of inducing effective cytotoxicity in malignant tissue and limited damage to the surrounding healthy tissues.[13] Therefore, PDT has superior properties compared with conventional cancer therapies such as chemotherapy and radiotherapy: it is selective, noninvasive, and has few side effects.[14,15]

The selectivity of the traditional PDT is due to the fact that the PS concentrates specifically within the malignant tissues, so when the light is directly focused on the lesion, it causes PDT reactive oxygen species (ROS) to be generated which results in cellular destruction of this specific domain. However, this ideal view is not often the case and many PS agents have limited affinity for tumor tissues and may cause skin photosensitivity or other side effects, as well as restriction for use in minimal doses of the drug.[16,17] In order to improve the affinity and thus the selectivity of the PDT, the PS can be conjugated covalently to an active carrier. This new paradigm is referred to as "third generation PDT" or selective photodynamic therapy (sPDT).[18] For example, Lafont and co-workers conjugated phthalocyanine PS to different monocarbohydrates as potential selective drugs for cancer cells due to their high energy consumption of monocarbohydrates (a readily available energy source).[18,19] sPDT was

Received: June 4, 2015
Published: August 11, 2015

DOI: 10.1021/acs.bioconjchem.5b00406
Bioconjugate Chem. 2015, 26, 1916−1922

also achieved by the encapsulation of the PS *meta*-tetra-(hydroxyphenyl)chlorin (m-THPC) to PEGylated liposomes bearing folic acid (as a cancer-targeting ligand) on their surface.[20] Rebane et al. targeted porphyrin-based PS to SST2 receptors or EGF receptors.[21] These three recent reports reflect the importance of finding selective and effective carriers in order to improve the PDT approach dramatically.

Peptide nucleic acid (PNA) is a nucleobase oligomer in which the entire backbone of pentose sugar and phosphate has been replaced by *N*-(2-aminoethyl)glycine units while preserving the original distances between the nucleobases.[22] The unique structure of the neutral peptide backbone and nucleobases renders the PNA with unique properties: (i) high chemical and biological stability, (ii) significantly greater stability of the PNA-DNA hybrid than double-stranded DNA (dsDNA) and, (iii) ability of peptide chemistry to conjugate many molecules of interest via the carboxylic group and/or amine group of the PNA. Thus, the conjugation of a short peptide such as a cell penetrating peptide (CPP) on one end of the PNA,[3,23−26] and a PS on the other, may provide an ideal chemical design for sPDT.

We have chosen Rose Bengal (RB) as a suitable PS for its conjugation to a 10 mer PNA. RB has many advantages including: (A) high yield of singlet oxygen generation (76%),[27] (B) well-established PS for PDT,[28−30] (C) low toxicity,[31−33] (D) good chemical and photostability,[34] (E) excitation wavelength at the visible spectrum,[35] (F) commercial availability and low cost, and (G) simple synthetic pathway for its conjugation.[36]

We have designed PNA-RB conjugates to which a PEGylated di-lysine (K-PEG-K) was attached to the PNAs C-terminus. The two lysines and the polyethylene glycol (PEG) linker are expected to provide the PNA conjugate with good water solubility and potentially improved cellular uptake. In addition, the two positive charges (lysine) separated by eight units of ethylene glycol were chosen in order to avoid PNA-DNA aggregation, a phenomenon we have observed with PNA-peptides where the peptide is highly charged (e.g., octa-lysine, data not shown).

Herein, we report the synthesis of PNA-RB conjugates and in vitro evaluation of these conjugates by irradiation with synthetic DNA substrates. Mechanistic studies indicate that lysines have a crucial role in the photoinduced DNA modulation. This remarkable lysine-dependent photoreaction may be used as a strategy to enhance selective PDT activity for future applications.

RESULTS AND DISCUSSION

In order to explore photomodulation of DNA by PNA-RB conjugates we initially synthesized 16-mer PNA conjugates with eight lysines at the C-terminus and Trp-RB or Gly-RB at the N-terminus. Previous work in our lab using thiazole orange (TO)-DNA conjugates showed that insertion of L-Trp adjacent to TO can induce plasmid DNA photocleavage, as opposed to Gly, where minimal photoinduced cleavage was observed.[37] In the presence of an indole ring (Trp) in the vicinity of the dye (TO), singlet oxygen could react with the indole ring to form an endoperoxide. In turn, this species leads to substantial DNA (plasmid) cleavage.

RB is a very potent singlet oxygen generator ($\Theta = 0.76$),[27] and for that reason, we decided to examine the photoactivity of two PNAs side by side: one containing Gly adjacent to RB and the other Trp adjacent to RB (Figure S1). Indeed, these two K_8−PNA (16mer)-amino acid-RB conjugates presented a similar photoreactivity, excluding the endoperoxide mechanism as the dominating one (Figure S1). Although both octa-lysine PNA conjugates showed high photoreactivity, DNA-PNA solutions were found to be unstable. Both single-stranded DNA (ssDNA) and the octa-Lysine PNA are highly soluble and stable separately, but when mixed, precipitates typically form within less than 1 h. We postulate that PNAs with eight positive charges (lysines) may form strong and nonspecific electrostatic interactions with the negatively charged DNA polymer. Heating and mixing the solution was found to be useful in slowing down aggregate formation, whereas buffer (e.g., PBS, TRIS) did not change or even increase the rate of aggregate formation. MALVERN measurements indicate that some aggregates are formed immediately and that their size is in the range of 100−400 nm (data not shown). In order to minimize the aggregation phenomenon significantly, 10-mer PNAs were synthesized to which K-PEG_8-K (K-PEG-K) was added to the C-terminus (Figure 1). The new design of

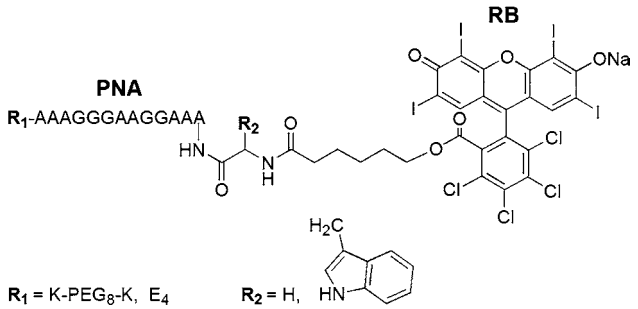

PNA-RB conjugate	Abbr.	Mass (theo.)	Mass (exp.)
K-PEG_8-K-GTCGCACGCG-Gly-RB	K-PEG-K-G-RB	4553.2	4548.8
K-PEG_8-K-GTCGCACGCG-Trp-RB	K-PEG-K-W-RB	4682.4	4681.1
E_4-GTCGCACGCG-Gly-RB	E_4-G-RB	4389.4	4385.0

Figure 1. PNA-RB sequences prepared and their corresponding Maldi-TOF MS assignments.

K-PEG-K-10mer-PNA has three main advantages: (1) it preserves the positive charge [2+], (2) it adds a hydrophilic character to the molecule (PEG) and, (3) it distances the positive charges via the PEG linker to minimize aggregation.

These PNA conjugates were found to be much more stable, although in the presence of the 50-mer ssDNA only a weak band of hybridized DNA-PNA was formed (Figure 2, upper band).

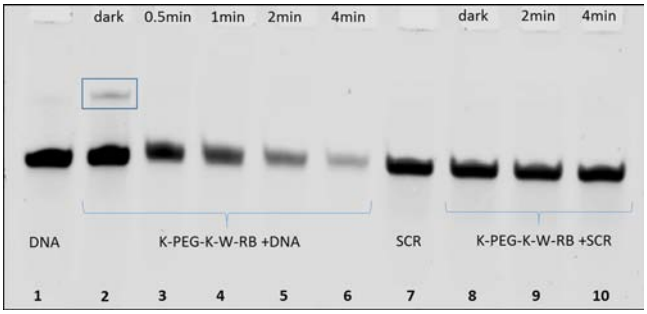

Figure 2. Irradiation of K-PEG-K-W-RB (45 μM, 8 equiv) with complementary and scrambled 50-mer ssDNAs. Lanes 1 and 7: 50-mer ssDNAs. Lanes 2−6: Complementary ssDNA and K-PEG-K-W-RB (45 μM, 8 equiv) in the dark and after 0.5, 1, 2, and 4 min of irradiation, respectively. Lanes 8−10: Scrambled ssDNA and K-PEG-K-W-RB (45 μM, 8 equiv) in the dark and after 2 and 4 min of irradiation, respectively. Irradiation was carried out at RT. All samples were prepared in a phosphate buffered saline (PBS) at pH = 7.4.

Nevertheless, a short irradiation of the solution showed high photoreactivity as evidenced by the gradual disappearance (as a

DOI: 10.1021/acs.bioconjchem.5b00406
Bioconjugate Chem. 2015, 26, 1916−1922

function of irradiation time) of the ssDNA band (Figure 2). The fact that a low percentage of hybridization is sufficient for high photoactivity (Figure 2, Lane 2) together with the disappearance of the ssDNA band (Figure 2, Lanes 3−6) may indicate a reversible mechanism where K-PEG-K-W-RB weakly interacts with the ssDNA during irradiation and reacts immediately. In addition, the scrambled ssDNA did not show any duplex formation and as a consequence did not undergo any photomodulation. Repeating this experiment with another DNA substrate that has the same central sequence but with different flanking regions (DNA-II) resulted in a similar photoreactivity (Figure S2).

Comparison between photoreactivity of K-PEG-K-W-RB and K-PEG-K-G-RB under identical conditions (i.e., PNA equivalents and irradiation time), showed that the PNA conjugate with Gly adjacent to RB is by far more active (Figure 3A). After 2 min

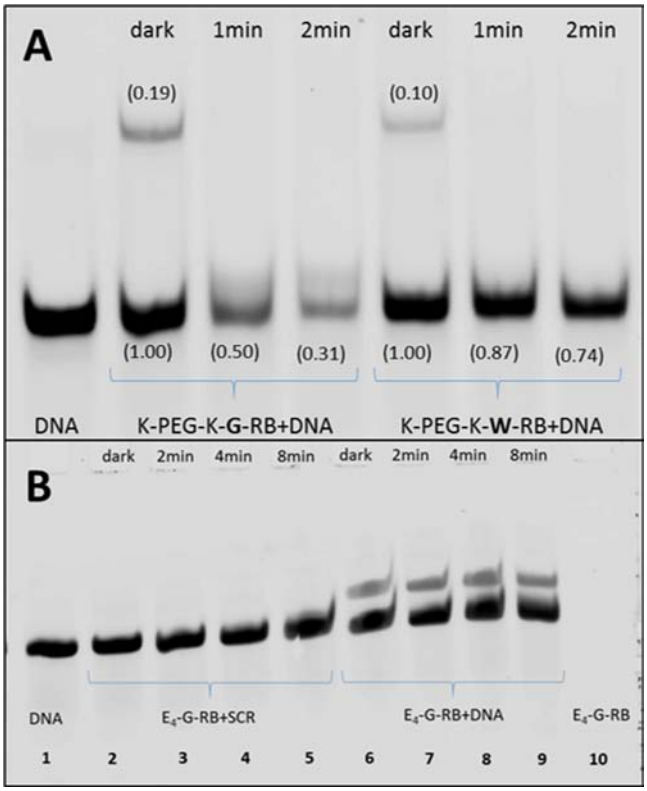

Figure 3. Panel A: Comparing photoreactivity of K-PEG-K-**G**-RB and K-PEG-K-**W**-RB (28 μM, 4 equiv) with a 50-mer ssDNA after 1 and 2 min of irradiation. The intensity of the ssDNA band over time and percentage of hybridization (upper band) were quantified and are presented in brackets. Panel B: Irradiation of E_4-G-RB with 50-mer ssDNA (complementary and scrambled sequences). Lane 1: 50-mer ssDNA. Lanes 2−5: Scrambled 50-mer ssDNA and E_4-G-RB (25 μM, 4 equiv) in the dark and after 2, 4, and 8 min irradiation, respectively. Lanes 6−9: Complementary 50-mer ssDNA and E_4-G-RB (25 μM, 4 equiv) in the dark and after 2, 4, and 8 min irradiation, respectively. Lane 10: only E_4-G-RB (25 μM, 4 equiv). Conditions as in Figure 2.

of irradiation, K-PEG-K-G-RB leads to 69% decrease in the intensity of the ssDNA band as opposed to 26% for K-PEG-K-W-RB. The difference in reactivity for these two PNA conjugates may be explained by quenching of RB fluorescence by L-Trp[36] (Figure S3) and by stronger hybridization (upper bands, Figure 3A) of the PNA conjugate containing Gly. In addition, the higher reactivity of K-PEG-K-G-RB further supports the insignificant contribution of the indole ring (via the endoperoxide mechanism) to the photoreactivity as described earlier (Figure S1). The high reactivity, in spite of relative weak hybridization (Figure 3), and the gradual disappearance of the ssDNA band may imply a cross-linking mechanism where the DNA-PNA cross-linking products do not run on the polyacrylamide gel. A common DNA modulation is related to singlet oxygen reactivity to guanine. Singlet oxygen reacts with guanine to form a 4,8-endoperoxide that is then decomposed to 8-oxo-guanine. In turn, spirominodihydantoin and guanidinohydantoin adducts of 8-oxo-G readily react with nucleophiles such as amines of L-lysine that are found in peptides and proteins.[38,39]

Singlet oxygen was found to have an important role in the mechanism of photoreaction by PNA-RB conjugates. Repeating the irradiation experiment with K-PEG-K-G-RB in D_2O resulted in higher DNA photomodulation (Figure 4). In addition, the

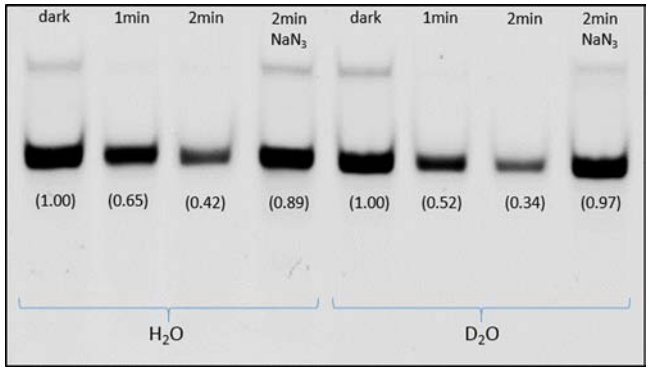

Figure 4. Comparing photoreactivity of K-PEG-K-**G**-RB (28 μM, 4 equiv) in H_2O and D_2O with a 50-mer ssDNA after 1 and 2 min of irradiation (lanes 2−3 and 6−7 for H_2O and D_2O, respectively). NaN_3 (2 mM) suppresses reaction (lanes 4 and 8 for H_2O and D_2O, respectively). The intensity of the ssDNA band over time and percentage of hybridization (upper band) were quantified and are presented in brackets. Irradiation was carried out at RT. Conditions as in Figure 2.

presence of NaN_3, a well-established singlet oxygen quencher,[40] suppressed the photoreaction.

To further elucidate this possible reaction pathway involving singlet oxygen and Lys (as nucleophile), a PNA conjugate with four glutamic acids (E_4) (instead of K-PEG-K) was synthesized. The negative charges are necessary to improve the solubility of the PNA conjugate and to allow its retention on the polyacrylamide gel. Hybridization of E_4-G-RB with the 50-mer ssDNA revealed that the RB is the main cause for the weak hybridization as noted earlier for the other PNA conjugates (Figure 2 and Figure 3A). Two equivalents of E_4-G (without RB) gave full hybridization whereas E_4-G-RB resulted in a relatively low hybridization, even when using a large excess (8 equiv) of E_4-G-RB (Figure S4).

Irradiation of the E_4-G-RB PNA conjugate (4 equiv) with 50-mer ssDNA under similar conditions did not result in any detectable photomodulation of the ssDNA, even after 8 min of irradiation (Figure 3B). This result supports the involvement of singlet oxygen and lysine in the photoinduced DNA modulation by PNA-RB conjugates.

The PNA conjugates are not stained by the Nancy-520 (Figure 3B, lane 10) nor by ethidium bromide. To visualize the PNA on the gel we followed the fluorescence of RB by scanning the gel directly without using the staining dye (Figure 5C).

Although a solution of ssDNA and K-PEG-K-G-RB is clear to the naked eye, according to the gel (Figure 5C, lane 2) and HPLC analysis (Figure 5A and D), there are aggregates even

DOI: 10.1021/acs.bioconjchem.5b00406
Bioconjugate Chem. 2015, 26, 1916−1922

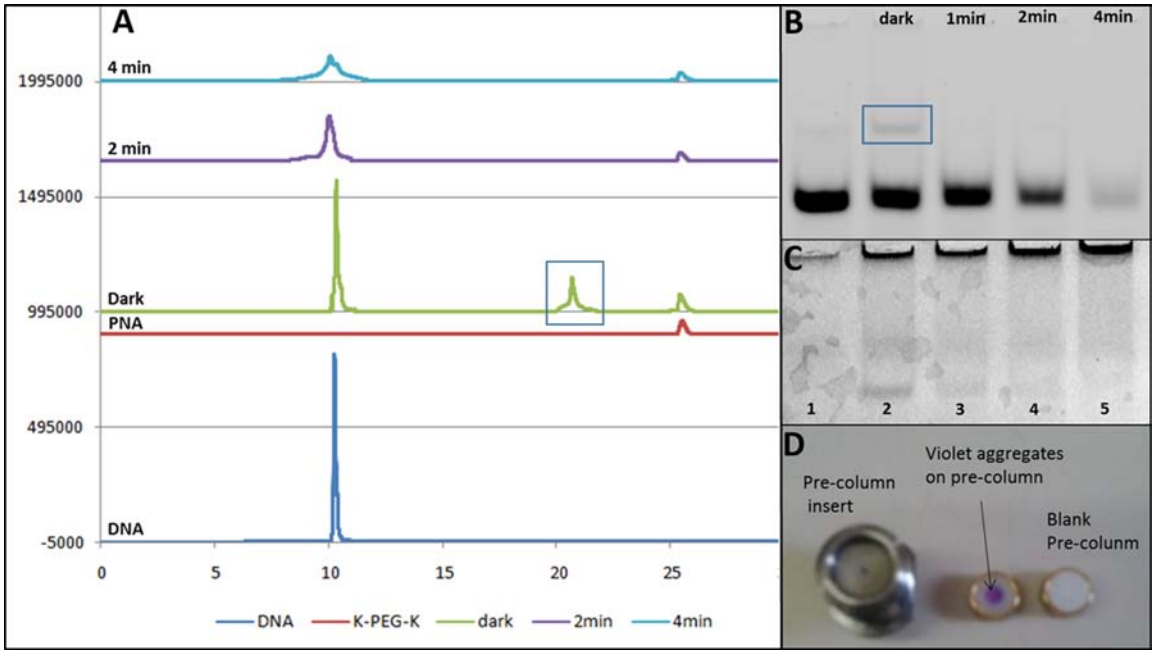

Figure 5. Photomodulation of 50-mer ssDNA (DNA-II) by K-PEG-K-G-RB (22 μM, 4 equiv). Panel A. HPLC chromatograms before and after irradiation (2 and 4 min) of K-PEG-K-G-RB (22 μM, 4 equiv) in the presence of 50-mer ssDNA (DNA-II). Panel B. Lane 1: 50-mer ssDNA (DNA-II). Lanes 2−5: complementary ssDNA and K-PEG-K-G-RB (22 μM, 4 equiv) in the dark and after 1, 2, and 4 min of irradiation, respectively. Gel was stained by Nancy-520 dye. Panel C. The same as in panel B, but image was taken without staining (RB fluorescence). Panel D. Violet aggregates of DNA:K-PEG-K-G-RB accumulate at the precolumn.

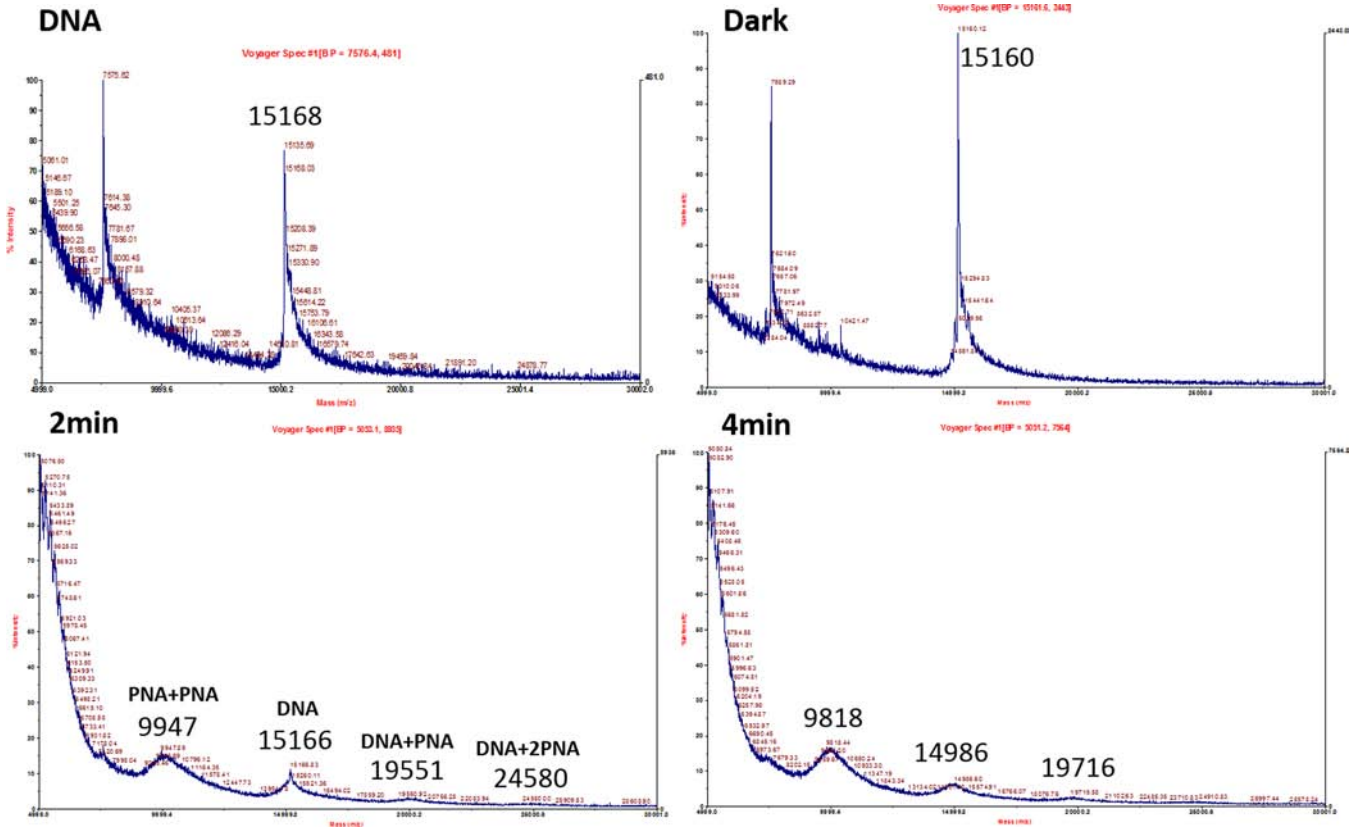

Figure 6. MALDI-TOF analysis of 50-mer ssDNA (DNA-II) and K-PEG-K-G-RB (22 μM, 4 equiv) in dark conditions and after 2 and 4 min of irradiation, respectively.

under dark conditions. Interestingly, when comparing the image taken using Nancy-520 (Figure 5B) to that without staining (Figure 5C), there is a good correlation between ssDNA band disappearance (Figure 5B) and the intensification of the band found at the top of the gel (in wells, Figure 5C), that is correlated to DNA-PNA aggregates. Therefore, we believe that

DOI: 10.1021/acs.bioconjchem.5b00406
Bioconjugate Chem. 2015, 26, 1916−1922

the disappearance of the ssDNA is a result of cross-linking to the K-PEG-K-G-RB, forming nanoparticles that are observed at the bottom of the wells. Further evidence for a photo-cross-linking mechanism was supported by direct injection of the irradiated samples to the HPLC (Figure 5A). The peaks of the 50-mer ssDNA and K-PEG-K-G-RB are observed at R_t = 10.2 and 25.5 min, respectively. Under dark conditions, the duplex peak DNA:PNA is observed at 20.5 min, and correlates well with the band associated with duplex DNA:PNA seen in the gel (Figure 5B, lane 2, boxed). After irradiation (2 and 4 min) the duplex peak disappeared and the ssDNA peak decreased dramatically. Moreover, the width of the 50-mer ssDNA peak has broadened, suggesting that other than aggregation, ssDNA is modified due to a photoinduced oxidation of the nucleobases. The residual ssDNA remaining after 2 and 4 min irradiation correlates well in both gel and HPLC (Figure 5A,B).

Support for DNA photoinduced modulation was corroborated by MALDI-TOF analysis. A solution of 50-mer ssDNA (DNA-II) and 4 equiv of K-PEG-K-G-RB was measured in dark conditions and after 2 and 4 min of irradiation (Figure 6). The results show that the main peak of the ssDNA (at 15 kDa) decreases dramatically over time. After 4 min of irradiation, the 50-mer ssDNA is not detectable; instead, a broad peak of masses appears (centered at ca. 15 kDa) that correlates with the smeared peak of the parent ssDNA detected by HPLC analysis (Figure 5A). In addition, after irradiation, broad peaks appear at ca. 9.9 kDa, 19.5 kDa, and 24.5 kDa that correspond to photoadducts of PNA-PNA, DNA-PNA, and DNA-$(PNA)_2$, respectively. This data further supports a model in which DNA-PNA photo-cross-linking induces aggregation in solution.

In summary, we have designed and synthesized PNA-RB conjugates as potent and sequence-specific photoinduced DNA modulators that are activated with visible light. We have provided evidence for a mechanism that involves the generation of singlet oxygen by RB photoactivation and the involvement of an amine (Lys) leading to DNA:PNA photo-cross-linking adducts. Based on the high photoreactivity of K-PEG-K-G-RB, we are currently designing new PNA-RB conjugates as potential candidates for sPDT.

EXPERIMENTAL PROCEDURES

Materials. Fmoc-PNA monomers were purchased from PolyOrg (USA) and used as received. Fmoc-NH-$(PEG)_8$-COOH was purchased from ChemPep inc. (USA). Amino acids (Fmoc-D-Lys-(BOC) and Fmoc-D-Glu-(OtBu)), solvents, and reagents for peptide chemistry were purchased from Tzamal D-Chem (Israel).

ssDNA. 50-mer synthetic DNAs were purchased from Sigma-Aldrich and used as received. These sequences are as follows: Fully complementary DNA (referred as "DNA"): 5′-TCCA-CCTCCTCCTTCTCGCGTGCGACGGAGCAAGCGCG-CTCCCAGCTCGC (underlined is the target area, complementary to the PNA-RB conjugate). Fully complementary DNA-II (referred as "DNA-II"): 5′-TCCACCTCCTCCTTC-TCGCGTGCGACGGAGCAAGCGCGCTCCCAGCTCGC. Scrambled DNA (referred as "SCR"): 5′-GCCGTGTCTCG-GCCCTCCTAACTCGCTCCTCGGCACCTCCAAGGCC-GACG.

Irradiation of PNA-RB Conjugate with ssDNA. For all irradiation experiments, a 50-mer DNA with a central region that is fully complementary to the PNA-RB conjugates was chosen. The solutions were prepared by adding ssDNA (20−50 μM) and PNA-RB conjugate (200−300 μM) to an Eppendorf tube containing water (molecular biology reagent, Sigma) in order to obtain the final desired concentrations. (1.6 mM phosphate buffered saline, 0.45 mM KCl, 23 mM NaCl, pH = 7.4, Sigma-Aldrich, USA). Typically, 3 μL of DNA (50 μM, 150 nmol) and 2 μL of PNA-RB conjugate (300 μM, 600 nmol, 4 equiv) were added to an Eppendorf tube containing 13 μL of water (final concentrations: ssDNA - 8.3 μM and PNA-RB - 33.3 μM).

Pre-irradiation, all the solutions were annealed (2 min at 90 °C followed by gradual cooling to RT). Irradiation was done with visible light generated from a 150 W halogen lamp (MRC, Israel) with a cutoff filter passing light between 450 and 800 nm which is in the region of RB absorption (Figure S5). This lamp has two fiber optic sieves that enable to aim the light source onto the sample. The Eppendorf tubes were positioned 1 cm away from the fiber optic. After irradiation, the loading buffer (Thermo Scientific, 6X DNA loading dye) was added to the irradiated samples and these were loaded in wells for PAGE.

Gel Electrophoresis. PAGE (19:1 acrylamide/bis-acrylamide, 11.5% cross-linking) was carried out in Tris-borate-EDTA buffer (TBEX0.5). Running conditions: 25 min at 200 V. The gels were stained with Nancy-520 (Sigma, USA) for 1 h and washed 5 min with DDW. The gel was scanned with gel imager (Typhoon FLA 9500) adjusting laser to 532 nm.

HPLC Analysis of Irradiated Samples. The PNA:DNA samples were analyzed on a RP-HPLC (Shimatzu LC2010) using a semipreparative C18 reverse-phase column (Phenomenex, Jupiter 300 A) at a flow rate of 4 mL/min. Mobile phase: 0.1% TFA in H_2O (A) and acetonitrile (B).

Initial − 90% A, 10% B. 15 min − 20% A, 80% B. 20 min − 20% A, 80% B. 20.01 min −90% A, 10% B. 30 min − stop.

Solid-Phase Synthesis of PNA-RB Conjugates. A RB derivative suitable for coupling to the amino terminus of the PNA was synthesized as previously reported using 6-bromohexanoic acid in water/acetone 1:1 (NMR-Figure S6).[36,41]

The PNA was synthesized on solid phase based on literature procedures with some modifications described as follows:[42]

The first monomer Fmoc-D-Lys-(BOC) or Fmoc-D-Glu-(OtBu) was coupled to the free hydroxyl groups of TGA-NovaSyn (Merck, Germany) resin using 10 equiv of the amino acid, 5 equiv of diisopropylcarbodiimide (DIC), and 0.1 equiv of 4-dimethylaminopyrimidine (DMAP) in dry DMF. Fmoc deprotection was done by stirring with 20% piperdine in DMF for 20 min followed by washing with DMF and methylene chloride alternately.

For a 10 μmol scale synthesis on TGA-NovaSyn resin (loading −0.25 mmol/g): 2-(1*H*-7-azabenzotriazol-1-yl)--1,1,3,3-tetramethyl uronium hexafluorophosphate methanaminium (HATU, 40 μmol), hydroxybenzotrilazole (HOBT, 40 μmol), diisopropylethylamine (DIPEA, 80 μmol), and Fmoc-amino acids/FmocNH-$(PEG)_8$-COOH/Fmoc-PNA monomers (40 μmol) were mixed in dry DMF (2 mL) for 5 min and the solution was then added to the amine functionalized resin and mixed for 50 min. The addition of RB-COOH at the N-terminus was done twice (same conditions). Cleavage of the final PNA product from the solid support was done in neat trifluoroacetic acid for 3 h. Diethyl ether was added and the precipitate was collected, dissolved in water, and lyophilized. The crude PNA was purified by RP-HPLC (Figure S7). The three PNA sequences were verified by MALDI-TOF MS (Figure 1). Final solutions were measured at 260 nm and calculated based on the extinction coefficients of the nucleobases.

ASSOCIATED CONTENT

Supporting Information

This material is free via the Internet at The Supporting Information is available free of charge on the ACS Publications website at DOI: 10.1021/acs.bioconjchem.5b00406.

DOI: 10.1021/acs.bioconjchem.5b00406
Bioconjugate Chem. 2015, 26, 1916−1922

HPLC chromatograms, absorption and emission spectra of PNA-RB conjugates, polyacrlylamide gels of PNA-RB/DNA, and NMR of RB-hexanoic acid (PDF)

AUTHOR INFORMATION

Corresponding Author

*E-mail: eylony@ekmd.huji.ac.il; Fax:+972-2-6757574; Tel: +972-2-6758692.

Notes

The authors declare no competing financial interest.

ACKNOWLEDGMENTS

This research was supported by the Israel Science Foundation (grant No. 480/13). E.Y. acknowledges the David R. Bloom Center for Pharmacy for financial support.

ABBREVIATIONS

RB, Rose Bengal; PNA, peptide nucleic acid; PS, photosensitizer; sPDT, selective photo dynamic therapy

REFERENCES

(1) Yoshimura, Y., Ito, Y., and Fujimoto, K. (2005) Interstrand photocrosslinking of DNA via p-carbamoylvinyl phenol nucleoside. *Bioorg. Med. Chem. Lett. 15*, 1299−1301.

(2) Fujimoto, K., Yoshimura, Y., Ikemoto, T., Nakazawa, A., Hayashi, M., and Saito, I. (2005) Photoinduced DNA end capping via N-3-methyl-5-cyanovinyl-2′-deoxyuridine. *Chem. Commun.*, 3177−3179.

(3) Cogoi, S., Codognotto, A., Rapozzi, V., Meeuwenoord, N., van der Marel, G., and Xodo, L. E. (2005) Transcription inhibition of oncogenic KRAS by a mutation-selective peptide nucleic acid conjugated to the PKKKRKV nuclear localization signal peptide. *Biochemistry 44*, 10510−10519.

(4) Kim, K.-H., Nielsen, P. E., and Glazer, P. M. (2007) Site-directed gene mutation at mixed sequence targets by psoralen-conjugated pseudo-complementary peptide nucleic acids. *Nucleic Acids Res. 35*, 7604−7613.

(5) Kim, Y., and Hong, I. S. (2008) PNA/DNA interstrand cross-links from a modified PNA base upon photolysis or oxidative conditions. *Bioorg. Med. Chem. Lett. 18*, 5054−5057.

(6) Qiu, Z., Lu, L., Jian, X., and He, C. (2008) A Diazirine-based nucleoside analogue for efficient DNA interstrand photocross-linking. *J. Am. Chem. Soc. 130*, 14398−14399.

(7) Nowak-Karnowska, J., Chebib, Z., Milecki, J., Franzen, S., and Skalski, B. (2014) Highly efficient fluorescent interstrand photo-crosslinking of DNA duplexes labeled with 5-fluoro-4-thio-2′-O-methyluridine. *ChemBioChem 15*, 2045−2049.

(8) Zdrowowicz, M., Michalska, B., Zylicz-Stachula, A., and Rak, J. (2014) Photoinduced single strand breaks and intrastrand cross-links in an oligonucleotide labeled with 5-bromouracil. *J. Phys. Chem. B 118*, 5009−5016.

(9) Sakamoto, T., Tanaka, Y., and Fujimoto, K. (2015) DNA photo-cross-linking using 3-cyanovinylcarbazole modified oligonucleotide with threoninol linker. *Org. Lett. 17*, 936−939.

(10) Op de Beeck, M., and Madder, A. (2012) Sequence specific DNA cross-linking triggered by visible light. *J. Am. Chem. Soc. 134*, 10737−10740.

(11) Deroo, S., Le Gac, S., Ghosh, S., Villien, M., Gerbaux, P., Defrancq, E., Moucheron, C., Dumy, P., and Kirsch-De Mesmaeker, A. (2009) Oligonucleotide duplexes with tethered photoreactive Ruthenium(II) complexes: Influence of the ligands and their linker on the photoinduced electron transfer and crosslinking processes of the two strands. *Eur. J. Inorg. Chem. 2009*, 524−532.

(12) Detty, M. R., Gibson, S. L., and Wagner, S. J. (2004) Current clinical and preclinical photosensitizers for use in photodynamic therapy. *J. Med. Chem. 47*, 3897−3915.

(13) Dougherty, T. J., Grindey, G. B., Fiel, R., Weishaupt, K. R., and Boyle, D. G. (1975) Photoradiation therapy. 2. Cure of animal tumors with hematoporphoryn and light. *J. Natl. Cancer Inst. 55*, 115−121.

(14) Alexiades-Armenakas, M. R., and Geronemus, R. G. (2003) Laser-mediated photodynamic therapy of actinic keratoses. *Arch. Dermatol. 139*, 1313−1320.

(15) Hayata, Y., Konaka, C., Takizawa, N., and Kato, H. (1982) Hematoporphyrin derivative and laser photoradiation in the treatment of lung-cancer. *Chest 81*, 269−277.

(16) De Rosa, F. S., and Bentley, M. (2000) Photodynamic therapy of skin cancers: Sensitizers, clinical studies and future directives. *Pharm. Res. 17*, 1447−1455.

(17) Hopper, C. (2000) Photodynamic therapy: a clinical reality in the treatment of cancer. *Lancet Oncol. 1*, 212−9.

(18) Zorlu, Y., Dumoulin, F., Bouchu, D., Ahsen, V., and Lafont, D. (2010) Monoglycoconjugated water-soluble phthalocyanines. Design and synthesis of potential selectively targeting PDT photosensitisers. *Tetrahedron Lett. 51*, 6615−6618.

(19) Lafont, D., Zorlu, Y., Savoie, H., Albrieux, F., Ahsen, V., Boyle, R. W., and Dumoulin, F. (2013) Monoglycoconjugated phthalocyanines: Effect of sugar and linkage on photodynamic activity. *Photodiagn. Photodyn. Ther. 10*, 252−259.

(20) Moret, F., Scheglmann, D., and Reddi, E. (2013) Folate-targeted PEGylated liposomes improve the selectivity of PDT with meta-tetra(hydroxyphenyl)-chlorin (m-THPC). *Photochem. Photobiol. Sci. 12*, 823−834.

(21) Starkey, J. R., Pascucci, E. M., Drobizhev, M. A., Elliott, A., and Rebane, A. K. (2013) Vascular targeting to the SST2 receptor improves the therapeutic response to near-IR two-photon activated PDT for deep-tissue cancer treatment. *Biochim. Biophys. Acta, Gen. Subj. 1830*, 4594−4603.

(22) Nielsen, P. E., Egholm, M., Berg, R. H., and Buchardt, O. (1991) Sequence-selective recognition of DNA by strand displacement with a thymine-substituted polyamide. *Science 254*, 1497−1500.

(23) Brognara, E., Fabbri, E., Aimi, F., Manicardi, A., Bianchi, N., Finotti, A., Breveglieri, G., Borgatti, M., Corradini, R., Marchelli, R., et al. (2012) Peptide nucleic acids targeting miR-221 modulate p27(Kip1) expression in breast cancer MDA-MB-231 cells. *Int. J. Oncol. 41*, 2119−2127.

(24) Deuss, P. J., Arzumanov, A. A., Williams, D. L., and Gait, M. J. (2013) Parallel synthesis and splicing redirection activity of cell-penetrating peptide conjugate libraries of a PNA cargo. *Org. Biomol. Chem. 11*, 7621−7630.

(25) Ivanova, G. D., Arzumanov, A., Abes, R., Yin, H., Wood, M. J. A., Lebleu, B., and Gait, M. J. (2008) Improved cell-penetrating peptide-PNA conjugates for splicing redirection in HeLa cells and exon skipping in mdx mouse muscle. *Nucleic Acids Res. 36*, 6418−6428.

(26) Yin, H., Betts, C., Saleh, A. F., Ivanova, G. D., Lee, H., Seow, Y., Kim, D., Gait, M. J., and Wood, M. J. A. (2010) Optimization of Peptide Nucleic Acid antisense oligonucleotides for local and systemic dystrophin splice correction in the mdx mouse. *Mol. Ther. 18*, 819−827.

(27) Lamberts, J. J. M., Schumacher, D. R., and Neckers, D. C. (1984) Novel rose-bengal derivatives - synthesis and quantum yield studies. *J. Am. Chem. Soc. 106*, 5879−5883.

(28) Borges Pereira Costa, A. C., Campos Rasteiro, V. M., Pereira, C. A., Rossoni, R. D., Junqueira, J. C., and Cardoso Jorge, A. O. (2012) The effects of rose bengal- and erythrosine-mediated photodynamic therapy on Candida albicans. *Mycoses 55*, 56−63.

(29) Panzarini, E., Inguscio, V., Fimia, G. M., and Dini, L. (2014) Rose Bengal acetate photodynamic therapy (RBAc-PDT) induces exposure and release of damage-associated molecular patterns (DAMPs) in human HeLa cells. *PLoS One 9*, e105778.

(30) Arboleda, A., Miller, D., Cabot, F., Taneja, M., Aguilar, M. C., Alawa, K., Amescua, G., Yoo, S. H., and Parel, J.-M. (2014) Assessment of Rose Bengal versus riboflavin photodynamic therapy for inhibition of fungal keratitis isolates. *Am. J. Ophthalmol. 158*, 64−70.

(31) Wachter, E., Dees, C., Harkins, J., Scott, T., Petersen, M., Rush, R. E., and Cada, A. (2003) Topical rose bengal: Pre-clinical evaluation of pharmacokinetics and safety. *Lasers Surg. Med. 32*, 101−110.

DOI: 10.1021/acs.bioconjchem.5b00406
Bioconjugate Chem. 2015, 26, 1916−1922

(32) Mousavi, S. H., Tavakkol-Afshari, J., Brook, A., and Jafari-Anarkooli, I. (2009) Direct toxicity of Rose Bengal in MCF-7 cell line: Role of apoptosis. *Food Chem. Toxicol. 47*, 855−859.
(33) Dini, L., inguscio, V., Tenuzzo, B., and Panzarini, E. (2010) Rose bengal acetate photodynamic therapy-induced autophagy. *Cancer Biol. Ther. 10*, 1048−1056.
(34) Lamberts, J. J. M., and Neckers, D. C. (1985) Rose bengal derivatives as singlet oxygen sensitizers. *Tetrahedron 41*, 2183−2190.
(35) Chang, C.-C., Yang, Y.-T., Yang, J.-C., Wu, H.-D., and Tsai, T. (2008) Absorption and emission spectral shifts of rose bengal associated with DMPC liposomes. *Dyes Pigm. 79*, 170−175.
(36) Carreon, J. R., Roberts, M. A., Wittenhagen, L. M., and Kelley, S. O. (2005) Synthesis, characterization, and cellular uptake of DNA-binding rose bengal peptidoconjugates. *Org. Lett. 7*, 99−102.
(37) Biton, A., Ezra, A., Kasparkova, J., Brabec, V., and Yavin, E. (2010) DNA Photocleavage by DNA and DNA-LNA Amino Acid-Dye Conjugates. *Bioconjugate Chem. 21*, 616−621.
(38) Solivio, M. J., Nemera, D. B., Sallans, L., and Merino, E. J. (2012) Biologically Relevant Oxidants Cause Bound Proteins To Readily Oxidatively Cross-Link at Guanine. *Chem. Res. Toxicol. 25*, 326−336.
(39) Johansen, M. E., Muller, J. G., Xu, X. Y., and Burrows, C. J. (2005) Oxidatively induced DNA-protein cross-linking between single-stranded binding protein and oligodeoxynucleotides containing 8-oxo-7,8-dihydro-2′-deoxyguanosine. *Biochemistry 44*, 5660−5671.
(40) Hasty, N., Merkel, P. B., Radlick, P., and Kearns, D. R. (1972) Role of Azide in Singlet Oxygen Reactions - Reaction of Azide with Singlet Oxygen. *Tetrahedron Lett. 13*, 49−52.
(41) Neckers, D. C., and Paczkowski, J. (1986) Rose Bengal derivatives. 15. Micro-organizational control of photochemical oxidants. *Tetrahedron 42*, 4671−4683.
(42) Nielsen, P. E. (2002) PNA technology. *Methods in molecular biology (Clifton, N.J.) 208*, 3−26.

DOI: 10.1021/acs.bioconjchem.5b00406
Bioconjugate Chem. 2015, 26, 1916−1922